Tellus (1992), *44B*, 106–113

Model calculations of night-time atmospheric OH

By Y. LU and M. A. K. KHALIL, *Global Change Research Center,*
Department of Environmental Science and Engineering,
Oregon Graduate Institute, Beaverton, OR 97006, USA

(Manuscript received 21 November 1990; in final form 13 May 1991)

ABSTRACT

The distribution of OH in the troposphere at night was obtained with a time-dependent photochemical model. At night, the major source of OH in the troposphere is the reaction between O_3 and night-time HO_2. More than 16% of night-time HO_2 is produced by the thermal dissociation of HO_2NO_2. The sinks of OH at night are the same as during day-time. The globally and seasonally averaged night-time OH concentration is about 1.3×10^4 molecules/cm^3, which is about two orders of magnitude smaller than the globally and seasonally averaged day-time OH concentration. Night-time OH concentrations appear to be most important in winter in the middle troposphere at middle latitudes, where about 10% of removal of gases resulting from reactions with OH occurs at night. We also calculated the night-time OH concentrations over a wide range of climatic conditions, from the last ice age to the pre-industrial era, and to the present. We found that the day-time OH concentrations do not change much during these transitions but the night-time OH concentrations may have decreased significantly in the transitions between the ice ages and the pre-industrial times and between the pre-industrial times and the present.

1. Introduction

The importance of OH for tropospheric photochemistry was first recognized by Weinstock (1969) and Levy (1971). Since then, much work has been done in determining the atmospheric OH concentration (for an overview, see Altshuller (1989)).

Probably because the concentrations of OH at night is too small to detect, or perhaps, because it makes a small contribution to global atmospheric chemistry, night-time OH has rarely been studied (Hard et al., 1986; Shirinzadeh et al., 1987). Nevertheless, OH exists at night and continues to react with many species and radicals in the atmosphere.

In this paper, we discuss the concentrations of OH at night calculated with a time-dependent photochemical model. Since the concentrations of many trace gases change with changing climate, we also examined the response of OH concentrations over a wide range of climatic conditions, from the last ice age to the present.

2. Basic OH chemistry

The primary production of OH, or the entire HO_x family, comes from the reaction between $O(^1D)$ and water vapor:

$$O(^1D) + H_2O \rightarrow OH + OH. \qquad (R1)$$

Reaction (R1) is effective only during day-time when the photodissociation of O_3 creates $O(^1D)$. At night, all photolysis stops and the reaction (R1) is no longer a source of OH. The only dominant source of OH in the unpolluted night-time atmosphere is the reaction between O_3 and night-time HO_2:

$$HO_2 + O_3 \rightarrow OH + O_2 + O_2. \qquad (R2)$$

Unlike day-time, night-time HO_2 is largely produced by the thermal dissociation of HO_2NO_2:

$$HO_2NO_2 + M \rightarrow HO_2 + NO_2 + M. \qquad (R3)$$

Similar to OH during day-time, at night, OH also reacts with a variety of trace gases and free radicals, among which carbon monoxide and methane are still the two most important species which significantly affect OH distributions:

$$OH + CO \rightarrow H + CO_2 \qquad (R4)$$

$$CH_4 + OH \rightarrow CH_3 + H_2O. \qquad (R5)$$

The resulting H atoms from reaction (R4) are mostly quenched by oxygen gas in the atmosphere to form hydroperoxyl radicals, HO_2,

$$H + O_2 + M \rightarrow HO_2 + M, \qquad (R6)$$

which can regenerate OH by reaction (R2). It should be emphasized that the reaction (R6) is no longer the largest source of HO_2 at night, according to our calculation (Lu and Khalil, 1991).

The reaction between CH_4 and OH initiates a complicated sequence of reactions (see, e.g., Logan et al. (1981)), which creates a series of organic compounds. These organics also affect atmospheric OH level directly or indirectly.

The reaction between two members of an odd-hydrogen family always removes at least one molecule of HO_x, thus being important losses of HO_x:

$$OH + HO_2 \rightarrow H_2O + O_2 \qquad (R7)$$

$$HO_2 + HO_2 \rightarrow H_2O_2 + O_2 \qquad (R8)$$

$$OH + H_2O_2 \rightarrow H_2O + HO_2. \qquad (R9)$$

In addition to the above reactions, the heterogeneous removal processes of the nitrogen-containing acids such as HNO_2, HNO_3, and HO_2NO_2, are also losses of HO_x since the major sources of these acids in the troposphere are:

$$OH + NO_2 + M \rightarrow HNO_3 + M \qquad (R10)$$

$$OH + NO + M \rightarrow HNO_2 + M \qquad (R11)$$

$$HO_2 + NO_2 + M \rightarrow HO_2NO_2 + M. \qquad (R12)$$

Besides O_3, NO is another source of the night-time OH, since the reaction between NO and HO_2 also produces OH:

$$HO_2 + NO \rightarrow OH + NO_2. \qquad (R13)$$

However, in the unpolluted atmosphere, NO decreases very rapidly after sunset when the primary source of NO resulting from the photodissociation of NO_2 disappears, leading to only a small production of the night-time OH.

3. The model and results

The temporal and spatial variation of a chemical reactive species can be expressed by the mass continuity equation:

$$\frac{\partial C_i}{\partial t} = P_i - L_i + \frac{\partial}{\partial z} K_z \frac{\partial C_i}{\partial z}, \qquad (1)$$

where C_i is the concentration of the ith species, t is time, z is altitude, P_i and L_i are the chemical production and loss terms, and K_z is the vertical eddy diffusivity.

By using the Eulerian-backward implicit finite different approximation and successive iterative processes, we numerically solve the mass continuity equations for 18 reactive species simultaneously to obtain the distributions of these species, including OH (for the detailed description, see Lu and Khalil (1991)). In summary, our photochemical model contains the information on the physical features of the atmosphere such as temperature, pressure, solar intensity and turbulent transport, as well as on chemical kinetic and photochemical data. The model consists of 58 chemical reactions and 28 species, among which the distributions of 10 species are specified to calculate the concentrations of another 18 species including OH and HO_2 (see Fig. 1). The concentrations of the 18 reactive species are calculated for different times of day, four seasons, and different latitudes and altitudes.

Fig. 2 shows the diurnal variations of the concentrations of OH at the surface of the earth and 6 km above the surface in summer and in winter at four latitudes. The difference between the maximum concentration of OH at noon and the minimum at dawn at the earth's surface is about a 10^6, which is much larger than the difference of about 10^2 at 6 km.

The averaged night-time OH concentration at a specific location in a season can be obtained by taking a time average of the concentrations of OH for the whole night, from sunset to sunrise. As shown in Fig. 3, the vertical profiles of

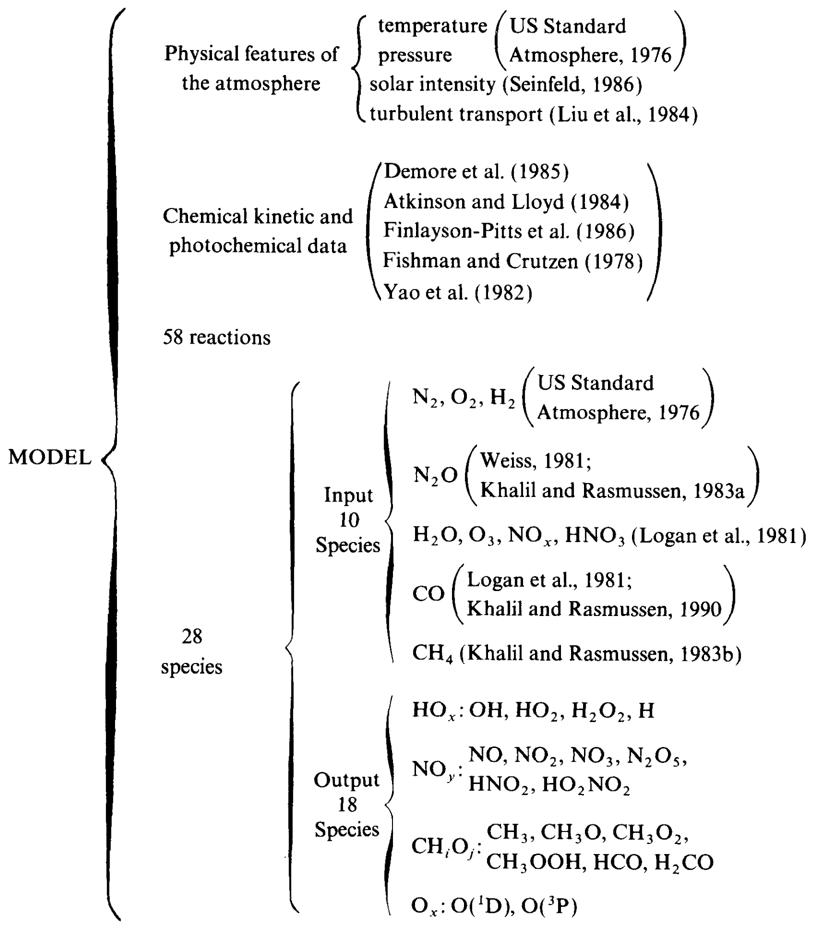

Fig. 1. Summary of our photochemical model.

the averaged night-time OH concentrations at different latitudes in different seasons have a common feature: the averaged night-time value first increases with height in the lower troposphere, reaches a maximum at around the middle troposphere, then decreases with height until it reaches a minimum at 10 or 11 km, and finally changes slightly with height at the top of the troposphere. This vertical structure of the averaged night-time OH concentration is mainly controlled by the vertical structures of the concentrations of O_3, HO_2NO_2, NO_2, CO, and CH_4. According to our calculation, more than 95% of the total night-time OH is produced by the reaction between O_3 and HO_2 and more than 60% of night-time HO_2 is generated by the thermal dissociation of HO_2NO_2, while CO and CH_4 consume large fractions of night-time OH (about 50% for CO and about 20% for CH_4) and O_3 and NO_2 remove almost all the night-time HO_2 (about 50% for O_3 and 45% for NO_2) (see Lu and Khalil (1991)). This figure also indicates that on average, the night-time OH concentration at the earth's surface is much lower than 10^5 molecules/cm^3, consistent with the conclusion that OH level is lower than 0.9×10^5 molecules/cm^3 (their detection limit) at night given by Shirinzadeh et al. (1987) from their OH measurements in ambient air.

By taking an average over altitude and latitude, we obtained the globally-averaged night-time OH concentration of 1.3×10^4 molecules/cm^3, with an

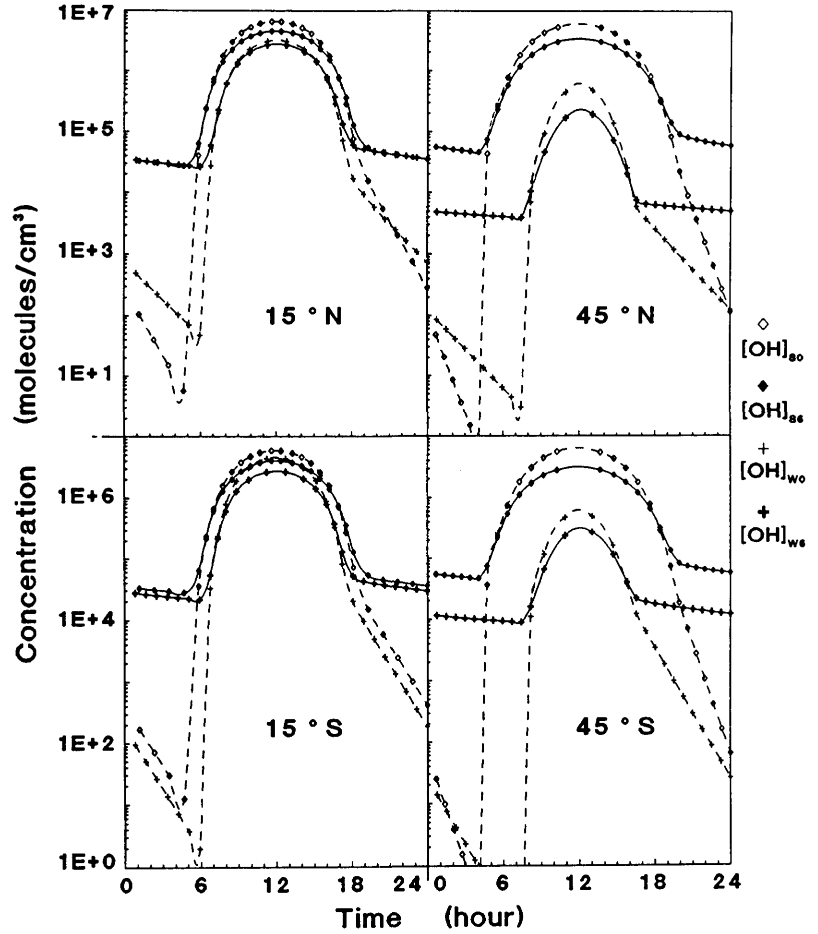

Fig. 2. Diurnal variations of the OH concentrations. $[\mathrm{OH}]_{\mathrm{S0}}$ and $[\mathrm{OH}]_{\mathrm{S6}}$ represent the OH concentrations at the earth's surface and at 6 km above the surface in summer; $[\mathrm{OH}]_{\mathrm{W0}}$ and $[\mathrm{OH}]_{\mathrm{W6}}$ designate the OH concentrations at the earth's surface and at 6 km above the surface in winter.

about 15% more abundance of night-time OH in the northern hemisphere than in the southern hemisphere, corresponding to the greater concentrations of O_3 and HO_2NO_2 in the northern hemisphere. On the whole, the averaged night-time OH concentration is about two orders of magnitude smaller than the averaged day-time OH concentration, 1.6×10^6 molecules/cm^3 (or 8.2×10^5 molecules/cm^3 of the globally and diurnally averaged OH concentration), which, calculated in the same model, agrees well with various OH calculations (Crutzen and Gidel, 1983; Khalil and Rasmussen, 1984; Logan et al., 1981; Prinn et al., 1987; Pinto and Khalil, 1991).

So far, the estimates of the night-time OH concentrations have been obtained with the model calculations. The next question is whether night-time OH is important for atmospheric chemistry. To answer this question, we defined the relative contribution of the night-time OH at the jth altitude in the ith season at the kth latitude, r_{kij}:

$$r_{kij} = \frac{\overline{[\mathrm{OH}^n]}_{kij} \cdot t_{ki}}{\overline{[\mathrm{OH}]}_{kij} \cdot 24}, \tag{2}$$

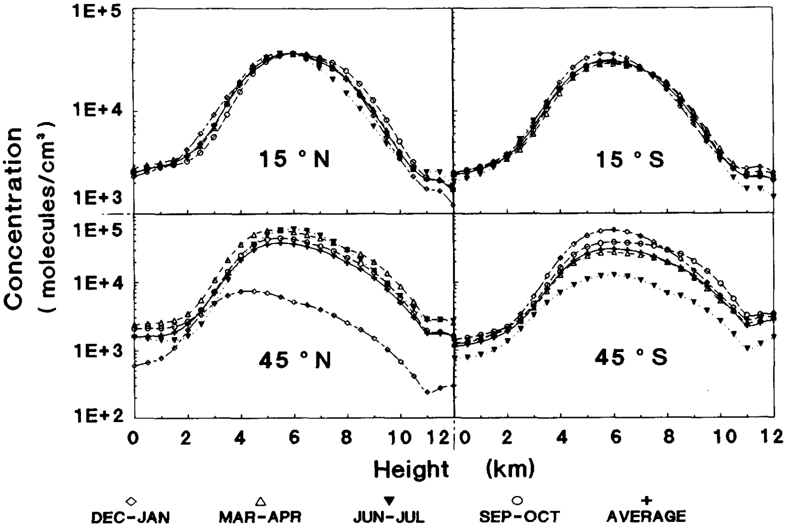

Fig. 3. Vertical profiles of the averaged night-time OH concentrations in 4 seasons and the seasonally-averaged night-time OH concentrations at 4 latitudes.

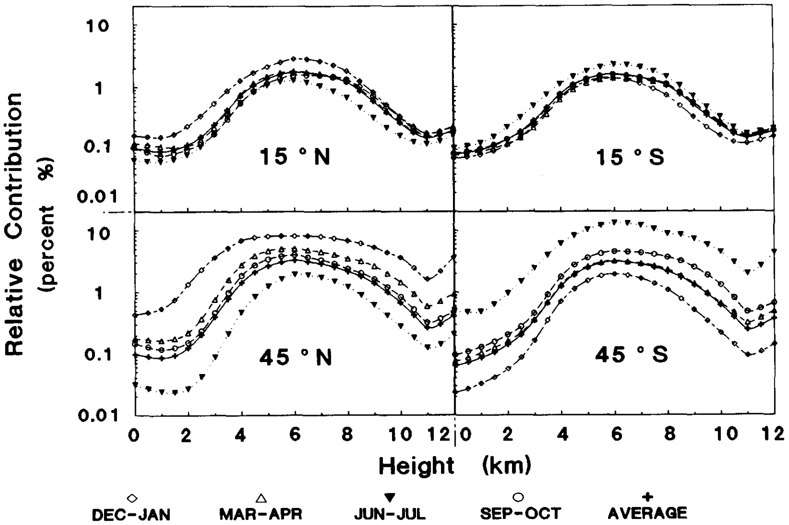

Fig. 4. Vertical profiles of the relative contribution of the night-time OH in 4 seasons at 4 latitudes (calculated by using eq. (2)) and those of seasonally averaged night-time OH at 4 latitudes (calculated by using eq. (3)).

where t_{ki} is the time from sunset to sunrise (h) in the ith season at the kth latitude; $\overline{[OH^n]}_{kij}$ is the averaged OH night-time concentration and $\overline{[OH]}_{kij}$ is the diurnally-averaged OH concentration. Similarly, the relative contributions of seasonally averaged night-time OH at the jth altitude and the kth latitude (r_{kj}), those of the vertically averaged night-time OH in the ith season (r_{ki}), and those of the seasonally and vertically averaged night-time OH at the kth latitude, r_k, were also defined by the following formulas:

$$r_{kj}=\frac{\sum_{i=1}^{4}\overline{[OH^n]}_{kij}\cdot t_{ki}}{\sum_{i=1}^{4}\overline{[OH]}_{kij}\cdot 24} \tag{3}$$

$$r_{ki}=\frac{\overline{[OH^n]}_{ki}\cdot t_{ki}}{\overline{[OH]}_{ki}\cdot 24} \tag{4}$$

$$r_{k}=\frac{\sum_{i=1}^{4}\overline{[OH^n]}_{ki}\cdot t_{ki}}{\sum_{i=1}^{4}\overline{[OH]}_{ki}\cdot 24}, \tag{5}$$

where $\overline{[OH^n]}_{ki}$ is the vertically-averaged night-time concentration of OH in the ith season at the kth latitude and $\overline{[OH]}_{ki}$ is the vertically and diurnally averaged concentration of OH in the same season at the same latitude. Fig. 4 shows the vertical profiles of the relative contributions of night-time OH in 4 seasons at 4 latitudes and those of seasonally averaged night-time OH at 4 latitudes. Generally, the values of the relative contributions of the averaged night-time OH, r_{kj}, are less than 0.5% in the lower and the upper troposphere, indicating that the night-time OH there contributes little to the chemical cycles of most trace gases in the troposphere. In contrast, because of the relatively larger values, r_{kj}, (about 3% in the middle latitudes and 2% in the tropics), the night-time OH in the middle troposphere is more important, especially at the midlatitudes in winter (13% at 45°S and 8% at 45°N, indicating that about 10% of the removal process resulting from reaction with OH occurs at night), not only because the intensity of the solar radiation is weak and the day-time is short, but also because there is more O_3 and HO_2NO_2 in these regions. On average, only about 1% of the total daily OH is produced at night in the whole troposphere.

Table 1. *Concentrations of tracers, number density of water vapor, and temperature at the surface of the Earth for 3 climatic conditions*[a]

Period	MT[b]	PE[b]	LGM[b]
CH_4 (ppbv)	1650	750	350
CO (ppbv)	110	57	28
H_2 (ppbv)	500	230	150
O_3 (ppbv)	22	14	12
NO_y[c] (ppbv)	0.1	0.05	0.05
N_2O (ppbv)	305	285	240
H_2O (molecule/cm^3)	3.32×10^{17}	3.32×10^{17}	2.44×10^{17}
temperature (°K)	288.15	288.15	283.15

[a] The data listed in the table are all taken from Pinto and Khalil (1990) except the number density of water vapor, computed from the formula for relative humidity given by Manabe and Wetherald (1967) and Clausius–Clapeyron equation.

[b] MT represents modern times; PE designates the pre-industrial era (about 200 years ago); LGM depicts the last glacial maximum (about 180,000 years ago).

[c] $NO_y = NO + NO_2 + NO_3 + 2\cdot N_2O_5 + HNO_2 + HNO_3 + HO_2NO_2$.

4. Climate and variability of night-time OH

Using our model calculations, we investigated OH levels over a wide range of climatic conditions, from the last glacial maximum (about 18,000 years ago), to the pre-industrial era, to modern times. The input data set for the 3 climatic periods are shown in Table 1, taken from Pinto and Khalil (1991). Fig. 5 shows the concentrations of the averaged day-time OH, the averaged night-time OH, and the averaged daily OH at the earth's surface. From this figure, one can see that the OH levels, on average, declined only slightly, although the concentrations of CO and CH_4 doubled from the last glacial maximum to the pre-industrial era as well as from the pre-industrial era to modern times, resulting from the compensation of the increasing levels of the source species of OH such as O_3 and NO_x for those of the sink species of OH such as CO and CH_4. This result is consistent with that given by Pinto and Khalil (1991). Since this paper is concerned with night-time OH, we emphasize that unlike the day-time OH, the night-time OH concentrations decreased significantly from the last glacial maximum to the present; the averaged night-time OH concentration in the last glacial maximum is about 3 times as large as that at present. As described before, the main sink of

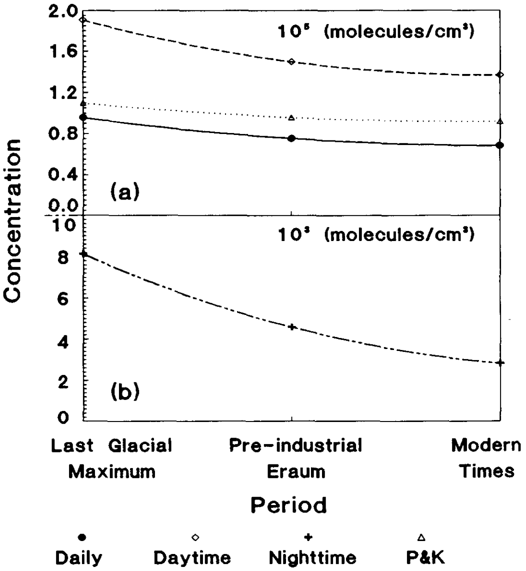

Fig. 5. The seasonally-averaged concentrations of the day-time OH and the daily OH at the earth's surface (a) and those of the night-time OH at the earth's surface (b) over a wide range of climatic condition, from the last glacial maximum (about 180,000 years ago), to the pre-industrial era (about 200 years ago), and to modern times (the present), where "Daily", "Day-time", and "Night-time" represent the concentrations of the averaged daily OH, the averaged daytime OH, and the averaged night-time OH, calculated from our photochemical model in this study, respectively, while "P&K" corresponds to the averaged daily OH concentrations calculated by Pinto and Khalil (1991).

night-time OH is CO, while the only significant source of night-time OH is the reaction between O_3 and night-time HO_2, which are largely produced by HO_2NO_2, one species of the NO_y family, and are removed by O_3 and NO_2, another species of NO_y. Thus, the trend of increasing night-time OH level due to increasing atmospheric O_3 level is offset by the trend of the decreasing night-time HO_2 level, resulting from the reaction between HO_2 and O_3. Similarly, enhancements of levels of HO_2NO_2 and NO_2, due to increasing atmospheric NO_y, compensate each other, leading to the trend of a slight increase of night-time OH. Consequently, the effects of increasing both O_3 and NO_y are attenuated and cancelled. In other words, the significant decrease of night-time OH arises mainly from the increase of CO and CH_4 from the last glacial maximum to the pre-industrial era and from the pre-industrial to the present.

5. Conclusion and discussion

Our model results give a globally and seasonally averaged night-time OH concentration of 1.3×10^4 molecules/cm^3 at present. However, the night-time OH concentration was much larger during ice ages than it is now; the averaged night-time OH concentration at the earth's surface in the last glacial maximum was about $3\times$ as large as at present. According to our calculations, the concentration of the night-time OH is dominated by the concentrations of O_3, HO_2NO_2, NO_2 and CO. The importance of the night-time OH is greatest in winter at middle latitudes in the middle troposphere, where there is more O_3 and HO_2NO_2, and the concentration of the dominant sink, CO, is small compared to that at the earth's surface. Our model results do not show NO as a significant source of night-time OH and the reaction between NO and HO_2 provides less than 5% of the total night-time OH, since in a clean atmosphere, NO is mainly produced by the photodissociation of NO_2 and after sunset the concentration of NO drops very quickly. Instead, the HO_2NO_2 can be seen as a major source of night-time OH, since HO_2NO_2 produces more than 60% of night-time HO_2 and the reaction between the resulting HO_2 and O_3 is the only significant source of night-time OH. It should be noted that our results do not conflict with the view that NO is an important source of night-time OH in urban areas, as suggested by Hard et al. (1986). Their measurements were made at an urban site, where NO may be directly emitted from fossil fuel combustion. Because the rate constant for the reaction between NO and HO_2 is much larger than that between O_3 and HO_2, the contribution to night-time OH from NO could be comparable to or even larger than that from O_3 in a polluted area.

Generally we conclude that the concentration of OH at night would be significantly larger in a polluted area where O_3 and NO_x are much more abundant than in a clean non-urban atmosphere. In addition, night-time OH was much more abundant during the ice ages compared to the present.

6. Acknowledgments

We thank R. A. Rasmussen, M. J. Shearer, W. Zhao, R. M. MacKay, and F. Moraes for helpful discussions. This project was supported in part by grants from the NSF (ATM-8811059, DPP-8717023, DPP-8820632, and DPP-8821320), and the Department of Energy (DE-FG06-85ER60313), and the resources of Andarz Co.

REFERENCES

Altshuller, 1989. Ambient air hydroxyl radical concentrations: measurements and model predictions. *J. Air Poll. Asso. 39*, 704–708.

Atkinson, R. and Lloyd, A. C. 1984. Evaluation of kinetic and mechanistic data for modeling of photochemical smog. *J. Phys. Chem. Ref. Data 13*, 315–444.

Crutzen, P. J. and Gidel, L. T. 1983. A two-dimensional photochemical model of the atmosphere, 2: The tropospheric budgets of the anthropogenic chlorocarbons CO, CH_4, CH_3Cl and the effect of various NO_x sources on tropospheric ozone. *J. Geophys. Res. 88*, 6641–6661.

DeMore, W. B., Margltan, J. J., Molina, M. J., Watson, R. T., Goldon, D. M., Hampson, R. F., Kurylo, M. J., Howard, C. J. and Ravishankara, A. R. 1985. Chemical kinetics and Photochemical data for use in stratospheric modeling. *JPL Publication* 85–87.

Finlayson-Pitts, B. J. and Pitts, Jr., J. N. 1986. *Atmospheric chemistry: Fundamentals and experimental techniques*, John Wiley & Sons, Inc, New York.

Fishman, J. and Crutzen, P. J. 1978. *The distribution of the hydroxyl radical in the troposphere*, Atmospheric Science, Paper no. 284, Dept. of Atmos. Science, Colorado State Univ., Fort Collins, Colorado.

Hard, T. M., Chan, C. Y., Mehrabzadeh, A. A., Pan, W. H. and O'Brien, R. J. 1986. Diurnal cycle of tropospheric OH. *Nature 322*, 617–620.

Khalil, M. A. K. and Rasmussen, R. A. 1983a. Increase and seasonal cycles of nitrous oxide in the earth's atmosphere. *Tellus 35B*, 161–169.

Khalil, M. A. and Rasmussen, R. A. 1983b. Sources, sinks, and seasonal cycles of atmospheric methane. *J. Geophys. Res. 88*, 5131–5144, 1983.

Khalil, M. A. K. and Rasmussen, R. A. 1984. Lifetime of methylchloroform (CH_3CCl_3), *Tellus 36B*, 317–332.

Khalil, M. A. K. and Rasmussen, R. A. 1990. The global cycle of carbon monoxide: trends and mass balance. *Chemosphere 20*, 227–242.

Levy, H. 1971. Normal atmosphere: Large radical and formaldehyde concentrations predicted, *Science 173*, 141–143.

Logan, J. A., Prather, M. J., Wosfy, S. C. and McElroy, M. B. 1981. Tropospheric chemistry: A global perspective. *J. Geophys. Res. 86*, 7210–7254.

Lu, Y. and Khalil, M. A. K. 1991. Tropospheric OH: model calculations of spatial, temporal, and secular variation. *Chemosphere 23*, 397–444.

Manabe, S. and Wetherald, R. T. 1967. Thermal equilibrium of the atmosphere with a given distribution of relative humidity. *J. Atmos. Sciences 24*, 241–259.

Pinto, J. P. and Khalil, M. A. K. 1991. The stability of tropospheric OH during ice ages, interglacial epoches, and modern times. *Tellus 43B*, 347–352.

Prinn, R., Cunnold, D., Rasmussen, R., Simmonds, P., Alyea, F., Crawford, A., Fraser, P. and Rosen, R. 1987. Atmospheric trends in methylchloroform and the global average for hydroxyl radical. *Science 238*, 945–950.

Seinfeld, J. H. 1986. *Atmospheric chemistry and physics of air pollution.* John Wiley & Sons, Inc.

Shirinzadeh, B., Wang, C. C. and Deng, D. Q. 1987. Diurnal variation of the OH concentration in ambient air. *Geophys. Res. Lett. 14*, 123–126.

US Standard Atmosphere, 1976. *National Oceanic and Atmospheric Administration, National Aeronautics and Space Administration and the United States Air Force.*

Weiss, R. F. 1981. The temporal and spatial distribution of tropospheric nitrous oxide. *J. Geophys. Res. 86*, 7185–7195.

Weinstock, B. 1969. Carbon monoxide: residence time in the atmosphere. *Science 166*, 224–225.

Yao, F., Wilson, I. and Johnston, H. 1982. Temperature-dependent ultraviolet absorption spectrum for dinitrogen pentoxide. *J. Phys. Chem. 86*, 3611.